Approaching conversion limit with all-dielectric solar cell reflectors

Sze Ming Fu, [1] Yi-Chun Lai,[3] Chi Wei Tseng,[1] Sheng Lun Yan,[1] Yan Kai Zhong,[1] Chang-Hong Shen,[2] Jia-Min Shieh,[2] Yu-Ren Li,[1] Huang-Chung Cheng,[1] Gou-chung Chi,[3]Peichen Yu,[3] and Albert Lin[1,*]

[1]*Department of Electronic Engineering, National Chiao-Tung Univeristy, Hsinchu, 30010, Taiwan*
[2]*National Device Laboratory(NDL), Hsinchu, 30010, Taiwan*
[3]*Department of Photonics, National Chiao-Tung Univeristy, Hsinchu, 30010, Taiwan*
[*]*hdtd5746@gmail.com*

Abstract: Metallic back reflectors has been used for thin-film and wafer-based solar cells for very long time. Nonetheless, the metallic mirrors might not be the best choices for photovoltaics. In this work, we show that solar cells with all-dielectric reflectors can surpass the best-configured metal-backed devices. Theoretical and experimental results all show that superior large-angle light scattering capability can be achieved by the diffuse medium reflectors, and the solar cell *J-V* enhancement is higher for solar cells using all-dielectric reflectors. Specifically, the measured diffused scattering efficiency (D.S.E.) of a diffuse medium reflector is >**0.8** for the light trapping spectral range (600nm-1000nm), and the measured reflectance of a diffuse medium can be as high as silver if the geometry of embedded titanium oxide(TiO_2) nanoparticles is optimized. Moreover, the diffuse medium reflectors have the additional advantage of room-temperature processing, low cost, and very high throughput. We believe that using all-dielectric solar cell reflectors is a way to approach the thermodynamic conversion limit by completely excluding metallic dissipation.

OCIS codes: (310.6845) Thin film devices and applications; (040.5350) Photovoltaic; (050.1940) Diffraction.

References and links

1. E. R. Martins, J. Li, Y. Liu, J. Zhou, and T. F. Krauss, "Engineering gratings for light trapping in photovoltaics: The supercell concept," Phys. Rev. B **86**(4), 041404 (2012).
2. H.-Y. Lin, Y. Kuo, C.-Y. Liao, C. C. Yang, and Y.-W. Kiang, "Surface plasmon effects in the absorption enhancements of amorphous silicon solar cells with periodical metal nanowall and nanopillar structures," Opt. Express **20**(S1), A104–A118 (2012).
3. C. Lin, N. Huang, and M. L. Povinelli, "Effect of aperiodicity on the broadband reflection of silicon nanorod structures for photovoltaics," Opt. Express **20**(1), A125–A132 (2012).
4. K. Q. Le, A. Abass, B. Maes, P. Bienstman, and A. Alù, "Comparing plasmonic and dielectric gratings for absorption enhancement in thin-film organic solar cells," Opt. Express **20**(1), A39–A50 (2012).
5. M. Y. Kuo, J. Y. Hsing, T. T. Chiu, C. N. Li, W. T. Kuo, T. S. Lay, and M. H. Shih, "Quantum efficiency enhancement in selectively transparent silicon thin film solar cells by distributed Bragg reflectors," Opt. Express **20**(S6), A828–A835 (2012).
6. K.-H. Hung, T.-G. Chen, T.-T. Yang, P. Yu, C.-Y. Hong, Y.-R. Wu, and G.-C. Chi, "Antireflective scheme for InGaP/InGaAs/Ge triple junction solar cells based on TiO2 biomimetic structures," in *IEEE Photovoltaic Specialists Conference*, (IEEE, 2012), 003322 - 003324.
7. O. Deparis and O. El Daif, "Optimization of slow light one-dimensional Bragg structures for photocurrent enhancement in solar cells," Opt. Lett. **37**(20), 4230–4232 (2012).
8. C. Battaglia, C.-M. Hsu, K. Söderström, J. Escarré, F. J. Haug, M. Charrière, M. Boccard, M. Despeisse, D. T. Alexander, M. Cantoni, Y. Cui, and C. Ballif, "Light trapping in solar cells: can periodic beat random?" ACS Nano **6**(3), 2790–2797 (2012).
9. Z. Yu and S. Fan, "Angular constraint on light-trapping absorption enhancement in solar cells," Appl. Phys. Lett. **98**(1), 011106 (2011).
10. M. Yang, Z. Fu, F. Lin, and X. Zhu, "Incident angle dependence of absorption enhancement in plasmonic solar cells," Opt. Express **19**(S4 Suppl 4), A763–A771 (2011).

#222520 - $15.00 USD Received 6 Oct 2014; revised 28 Nov 2014; accepted 20 Dec 2014; published 26 Jan 2015

11. X. Sheng, S. G. Johnson, J. Michel, and L. C. Kimerling, "Optimization-based design of surface textures for thin-film Si solar cells," Opt. Express **19**(S4 Suppl 4), A841–A850 (2011).
12. W. E. I. Sha, W. C. H. Choy, and W. C. Chew, "Angular response of thin-film organic solar cells with periodic metal back nanostrips," Opt. Lett. **36**(4), 478–480 (2011).
13. S. Pillai, F. J. Beck, K. R. Catchpole, Z. Ouyang, and M. A. Green, "The effect of dielectric spacer thickness on surface plasmon enhanced solar cells for front and rear side depositions," J. Appl. Phys. **109**(7), 073105 (2011).
14. U. W. Paetzold, E. Moulin, B. E. Pieters, R. Carius, and U. Rau, "Design of nanostructured plasmonic back contacts for thin-film silicon solar cells," Opt. Express **19**(S6 Suppl 6), A1219–A1230 (2011).
15. U. W. Paetzold, E. Moulin, D. Michaelis, W. Bottler, C. Wächter, V. Hagemann, M. Meier, R. Carius, and U. Rau, "Plasmonic reflection grating back contacts for microcrystalline silicon solar cells," Appl. Phys. Lett. **99**(18), 181105 (2011).
16. A. Naqavi, K. Söderström, F.-J. Haug, V. Paeder, T. Scharf, H. P. Herzig, and C. Ballif, "Understanding of photocurrent enhancement in real thin film solar cells: towards optimal one-dimensional gratings," Opt. Express **19**(1), 128–140 (2011).
17. J. N. Munday and H. A. Atwater, "Large integrated absorption enhancement in plasmonic solar cells by combining metallic gratings and antireflection coatings," Nano Lett. **11**(6), 2195–2201 (2011).
18. S. A. Mann, R. R. Grote, R. M. Osgood, and J. A. Schuller, "Dielectric particle and void resonators for thin film solar cell textures," Opt. Express **19**(25), 25729–25740 (2011).
19. C. Lin and M. L. Povinelli, "Optimal design of aperiodic, vertical silicon nanowire structures for photovoltaics," Opt. Express **19**(S5 Suppl 5), A1148–A1154 (2011).
20. H.-H. Li, P.-Y. Yang, S.-M. Chiou, H.-W. Liu, and H.-C. Cheng, "A novel coaxial-structured amorphous-silicon p-i-n solar cell with Al-doped ZnO nanowires," Elecron. Dev. Lett. **32**(7), 928–930 (2011).
21. T. Lanz, B. Ruhstaller, C. Battaglia, and C. Ballif, "Extended light scattering model incorporating coherence for thin-film silicon solar cells," J. Appl. Phys. **110**(3), 033111 (2011).
22. N. Lagos, M. M. Sigalas, and E. Lidorikis, "Theory of plasmonic near-field enhanced absorption in solar cells," Appl. Phys. Lett. **99**(6), 063304 (2011).
23. B.-J. Kim and J. Kim, "Fabrication of GaAs subwavelength structure (SWS) for solar cell applications," Opt. Express **19**(S3 Suppl 3), A326–A330 (2011).
24. F.-J. Haug, K. Söderström, A. Naqavi, and C. Ballif, "Resonances and absorption enhancement in thin film silicon solar cells with periodic interface texture," J. Appl. Phys. **109**(8), 084516 (2011).
25. J. Grandidier, D. M. Callahan, J. N. Munday, and H. A. Atwater, "Light absorption enhancement in thin-film solar cells using whispering gallery modes in dielectric nanospheres," Adv. Mater. **23**(10), 1272–1276 (2011).
26. F. J. Beck, S. Mokkapati, and K. R. Catchpole, "Light trapping with plasmonic particles: beyond the dipole model," Opt. Express **19**(25), 25230–25241 (2011).
27. S. Zanotto, M. Liscidini, and L. C. Andreani, "Light trapping regimes in thin-film silicon solar cells with a photonic pattern," Opt. Express **18**(5), 4260–4274 (2010).
28. Z. Yu, A. Raman, and S. Fan, "Fundamental limit of nanophotonic light trapping in solar cells," Proc. Natl. Acad. Sci. U.S.A. **107**(41), 17491–17496 (2010).
29. Z. Yu, A. Raman, and S. Fan, "Fundamental limit of light trapping in grating structures," Opt. Express **18**(S3 Suppl 3), A366–A380 (2010).
30. K. Söderström, F.-J. Haug, J. Escarré, O. Cubero, and C. Ballif, "Photocurrent increase in n-i-p thin film silicon solar cells by guided mode excitation via grating coupler," Appl. Phys. Lett. **96**(21), 213508 (2010).
31. X. Sheng, S. G. Johnson, L. Z. Broderick, J. Michel, and L. C. Kimerling, "Integrated photonic structures for light trapping in thin-film Si solar cells," Appl. Phys. Lett. **100**(11), 111110 (2012).
32. Y.-C. Lee, C.-F. Huang, J.-Y. Chang, and M.-L. Wu, "Enhanced light trapping based on guided mode resonance effect for thin-film silicon solar cells with two filling-factor gratings," Opt. Express **16**(11), 7969–7975 (2008).
33. J. Foley, S. Young, and J. Phillips, "Symmetry-protected mode coupling near normal incidence for narrow-band transmission filtering in a dielectric grating," Phys. Rev. B **89**(16), 165111 (2014).
34. J. M. Foley, A. M. Itsuno, T. Das, S. Velicu, and J. D. Phillips, "Broadband long-wavelength infrared Si/SiO_2 subwavelength grating reflector," Opt. Lett. **37**(9), 1523–1525 (2012).
35. S. Hänni, G. Bugnon, G. Parascandolo, M. Boccard, J. Escarré, M. Despeisse, F. Meillaud, and C. Ballif, "High-efficiency microcrystalline silicon single-junction solar cells," Prog. Photovolt. Res. Appl. **21**, 821–826 (2013).
36. B. Lipovšek, J. Krč, O. Isabella, M. Zeman, and M. Topič, "Modeling and optimization of white paint back reflectors for thin-film silicon solar cells," J. Appl. Phys. **108**(10), 103115 (2010).
37. J. E. Cotter, "Optical intensity of light in layers of silicon with rear diffuse reflectors," J. Appl. Phys. **84**(1), 618–624 (1998).
38. B. G. Lee, P. Stradins, D. L. Young, K. Alberi, T.-K. Chuang, J. G. Couillard, and H. M. Branz, "Light trapping by a dielectric nanoparticle back reflector in film silicon solar cells," Appl. Phys. Lett. **99**, 064101 (2011).
39. O. Berger, D. Inns, and A. G. Aberle, "Commercial white paint as back surface reflector for thin-film solar cells," Sol. Energ. Mat. Sol. C. **91**(13), 1215–1221 (2007).
40. J. E. Cotter, R. B. Hall, M. G. Mauk, and A. M. Barnett, "Light Trapping in Silicon-Film^{TM} Solar Cells with Rear Pigmented Dielectric Reflectors," Prog. Photovolt. Res. Appl. **7**(4), 261–274 (1999).
41. O. Kunz, Z. Ouyang, S. Varlamov, and A. G. Aberle, "5% efficient evaporated solidphase crystallised Polycrystalline silicon thin-film solar cells," Prog. Photovolt. Res. Appl. **17**(8), 567–573 (2009).
42. A. Basch, F. J. Beck, T. Söderström, S. Varlamov, and K. R. Catchpole, "Combined plasmonic and dielectric rear reflectors for enhanced photocurrent in solar cells," Appl. Phys. Lett. **100**, 243903 (2012).

#222520 - $15.00 USD Received 6 Oct 2014; revised 28 Nov 2014; accepted 20 Dec 2014; published 26 Jan 2015

43. C.-Y. Fang, Y.-L. Liu, Y.-C. Lee, H.-L. Chen, D.-H. Wan, and C.-C. Yu, "Nanoparticle stacks with graded refractive indices enhance the omnidirectional light harvesting of solar cells and the light extraction of light-emitting diodes," Adv. Mater. **23**, 1412–1421 (2013).
44. A. Goetzberger, "Optical confinement in thin Si-solar cells by diffuse back reflectors," in *15th IEEE Photovoltaic Specialist Conference*, (IEEE, 1981), 867–870.
45. A. Kitait, *Principles of Solar Cells, LEDs and Diodes: The role of the PN junction* (John Wiley & Sons, 2011).
46. Rsoft, *Rsoft CAD User Manual,* 8.2 ed. (Rsoft Design Group, 2010).
47. A. Lin, Y.-K. Zhong, and S.-M. Fu, "The effect of mode excitations on the absorption enhancement for silicon thin film solar cells," J. Appl. Phys. **114**(23), 233104 (2013).

1. Introduction

Solar cell back reflectors play an important part in nanophotonic light trapping [1–30]. The reflectors, in fact, serve dual roles. One is high reflectivity, and the other one is efficient light scattering. The strong angular light scattering and strong non-specular diffraction is preferable because this facilitates total internal reflection (TIR) and thus extends the effective optical path length. Metallic back reflectors have long been used for the solar industry. Aluminum reflectors are very common due to its lower cost and compatible to IC process technology. Silver reflectors are used in some cases, especially when surface plasmon is needed for enhanced near-field and far-field absorption enhancement [2, 4, 10, 13–15, 17, 22, 26]. The drawbacks of metallic back reflectors are severe metal absorption. Even for high reflectivity metal such as silver, significant absorption still degrade the solar cell efficiency. The drawback might be compensated by the fact that the surface plasmonic light trapping enhances the light scattering, though recent study suggests that the advantage by the plasmonic light scattering only barely compensates absorption [4, 13]. Dielectric mirrors have been proposed as the alternatives. This includes distributed Bragg reflectors(DBR) [5, 7, 31], high index contrast grating(HCG) [32–34], and diffuse medium reflectors [35–44]. The dielectric mirror in general has minimized absorption loss, but using dielectric reflectors eliminates the possibility of plasmonic photovoltaics. Among different kinds of dielectric mirrors, DBR is too costly for photovoltaics. This is because The distributed reflectors (DBR) generally require at least >10 depositions of alternating layers to achieve high reflectance. This adds cost to optoelectronic devices by lowering the throughput [45]. HCG has not been successfully implemented in solar cells because wide-bandgap transparent materials normally have a refractive index < 3 and therefore it is difficult to form a high index contrast grating. In this work, we show that diffuse medium reflectors, in fact, are promising for solar cells. The experimental work on thin-film solar cells is conducted, using amorphous silicon solar cells, to demonstrate the effectiveness of nanophotonic light trapping by diffuse medium mirrors. Simulation and angular emission measurement also confirm the superiority of diffuse mirrors, in terms of efficiency enhancement, over conventional metallic aluminum or silver reflectors.

2. Problem set-up: theoretical, experimental, and angular power measurement

In order to have thorough insight into diffuse medium reflectors, both theoretical and experimental works are conducted.

Firstly, theoretical analysis based on eigenmode expansion is used to study the angular scattering behaviors for various metallic back reflectors and diffuse medium reflectors. This is important because the angular scattering affects the solar cell light trapping. The material parameters are from Rsoft material database [46]. Although this work uses amorphous silicon as an example, the usefulness of diffuse medium reflectors is not diminished for solar cells made of other inorganic semiconductors. This is because the similar far-field light scattering, waveguiding, and guided mode excitation nature in these inorganic solar cells. As a result, which inorganic semiconductor is used as an example to demonstrate the effectiveness of diffuse medium reflectors is actually not critical. For organic solar cells, the white diffuse paint can be easily incorporated into the devices due to the low-temperature process nature of the organic device fabrication. Nonetheless, the near-field enhancement of plasmonic resonances is extremely efficient in ultra-thin organic solar cells, and therefore it is not necessary that diffuse medium reflectors can surpass their metallic counterparts. Detailed

#222520 - $15.00 USD Received 6 Oct 2014; revised 28 Nov 2014; accepted 20 Dec 2014; published 26 Jan 2015

study and comparison for dielectric paints and metallic nano-particles employed in organic solar cells should be conducted, before conclusions can be made. The calculation method is based on rigorously coupled wave analysis(RCWA) implemented by Rsoft DiffractMOD. The polarization angle is 45° and therefore the result is the average of s- and p-polarization. The eigen-mode expansion method generally decouples the reflected light into different propagation directions, corresponding to different diffraction orders. The reflected power is, usually, strongest at specular direction (0th order). Nonetheless, for nanophotonic light trapping, the higher order diffracted power, i.e. diffused power, is preferable.

After theoretical study, experimental evidence on real solar cells with various reflectors is provided. The amorphous silicon p-i-n solar cell is used to demonstrate the efficiency enhancement of solar cells with different back reflectors. In this study, in addition to diffuse medium reflectors, silver(Ag), aluminum(Al), nickel(Ni), and titanium(Ti) are used to assess the performance of different metal reflectors. Silver is among the highest conductivity metals and has surface plasmonic resonance wavelength in the visible spectrum which can facilitate solar cell absorption enhancement. Aluminum is very common in integrated circuit(IC) processing and has a reasonably high conductivity. A high conductivity is the key to reducing the metallic dissipation. Aluminum also has significantly lower cost than silver. For completeness, Ni and Ti is also included since they are also very common in clean rooms for semiconductor device processing, though their conductivities are lower.

Finally, the total reflected power(R_{tot}), the specular reflected power(R_{spec}), and the diffused reflected power($R_{diffuse}$) for various reflectors are measured. The total reflectance for diffuse medium reflectors used in this study can be comparable to silver, especially at long wavelength where light trapping is essential. In fact, the reflectance can be even higher if the pigment dimension, shape, and the pigment volume concentration (PVC) can be further optimized [35, 36]. Here the diffuse medium is shown to provide the measured reflectance close to one over broad spectral range. In addition, the specular and diffused power measurement further confirms the superior light scattering property of diffuse medium reflectors where its ultra-low specular reflection confirms its strong light scattering property.

3. Theoretical result based on coupled mode theory: dielectric mirror and the best-configured metallic mirrors

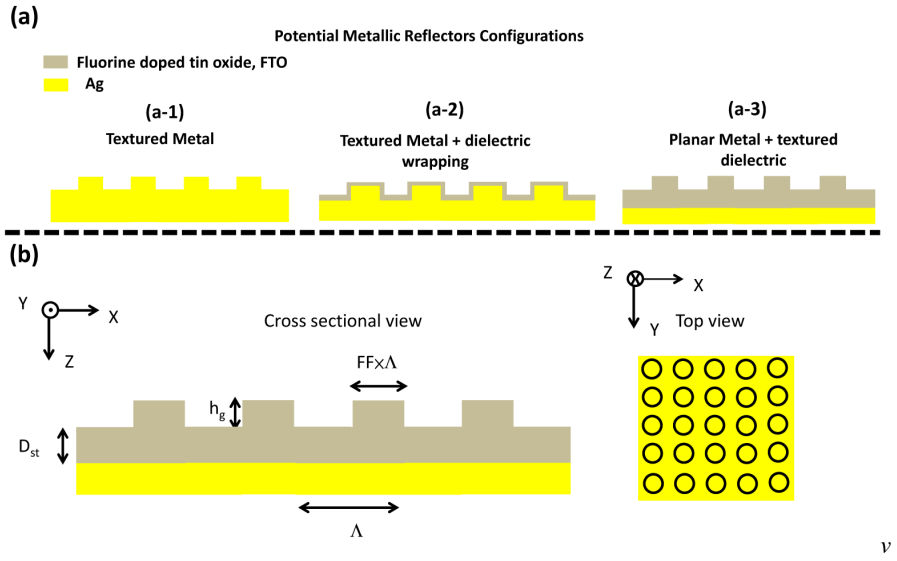

Fig. 1. Illustration of the simulation structure for silver metallic reflectors for solar cells. (a) different potential configurations of metallic reflectors for solar cells [47]. (b) The best-configured metallic mirror configuration for solar cell application, which is employed in this study.

#222520 - $15.00 USD Received 6 Oct 2014; revised 28 Nov 2014; accepted 20 Dec 2014; published 26 Jan 2015

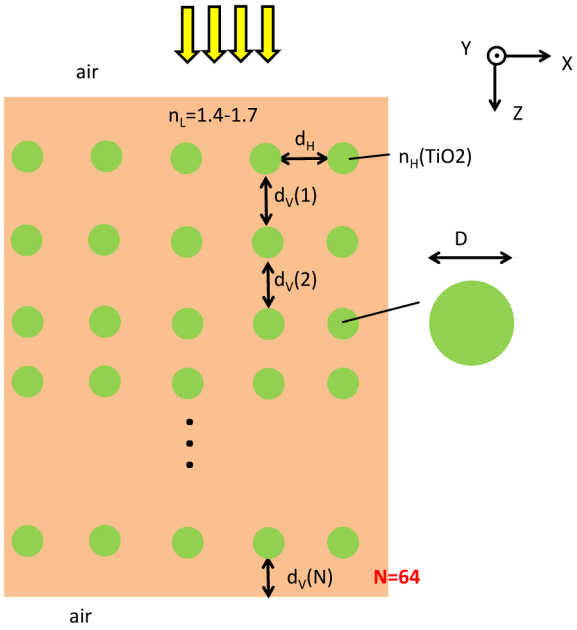

Fig. 2. Illustration of the simulation structure for white paint diffuse medium reflectors.

The structure for metallic reflectors used in this study is plotted Fig. 1(b). There are actually several different potential configurations for metallic mirrors for solar cells as shown in Fig. 1(a). The texture on the metal itself without a dielectric spacer, i.e. Figure 1(a-1) tends to result in severe metallic absorption. The textured metal with a dielectric wrapping in Fig. 1(a-2) is not as efficient as Fig. 1(a-3) where the structure is a planar metallic mirror with a textured dielectric spacer [47]. The flat metal reflector with a textured dielectric layer illustrated in Fig. 1(a-3) is, therefore, employed in this study because this is the most-efficient configuration for solar cell light trapping employing metallic mirrors [47]. The detailed dimensions for Fig. 1(a-3) are illustrated in Fig. 1(b). For diffuse medium reflectors, a white paint reflector is used [35, 36]. The titanium oxide (TiO_2) embedded in a lower index host material is formed to achieve so-called white reflective paint. In the simulation structure, the TiO_2 nanoparticles are random in z-direction and periodic in x- and y-direction. The one-dimensional randomness in z-direction has been used previously to study the diffuse medium [36]. This captures the essential physics of disordered media since z-direction is the primary wave propagation direction, and its randomness affects the light scattering property most significantly. In addition, true wave optics formulation for randomness in all of the three dimensions is in practice impossible to realize due to the algorithm and memory/center processing unit(CPU) limitation. The consistent high reflectance for both of the experimental and theoretical results confirms the validity of using one-dimensional randomness [36] for the purpose here. The geometry for the silver metallic reflector in Fig. 1(b) is Λ = 500nm, D_{st} = 187nm, FF = 0.38, and h_g = 194nm. The geometry for the white paint diffuse medium reflectors in Fig. 2 is d_H = 92 nm and D = 511 nm. A genetic algorithm is used to select the geometry to maximize the total reflectance for the metallic and diffuse medium mirrors. For white paint diffuse medium, the resulting geometry (D~500nm) is consistent with our commercial white paint confirmed with the vendor. It is also confirmed that the embedded nano-particles in this commercial white paint are indeed TiO_2.

The eigenmode expansion is a useful method to study the scattering properties of different back reflectors. The formulation is based on expanding the electromagnetic field by different eigen modes. Different modes correspond to the power coupled into different directions. Helmholtz equation for eigen mode expansion can generally be written as

#222520 - $15.00 USD Received 6 Oct 2014; revised 28 Nov 2014; accepted 20 Dec 2014; published 26 Jan 2015

$$\nabla^2 E(x,z) + \omega^2 \mu\varepsilon E(x,z)$$
$$= \nabla^2 \left[E_{inc} exp(jk_{inc} z) + \sum_i b_i(z) exp(jk_{x,i} x) \right] \quad (1)$$
$$+ \omega^2 \mu\varepsilon \left[E_{inc} exp(jk_{inc} z) + \sum_i b_i(z) exp(jk_{x,i} x) \right]$$

where the Helmholtz equation is written in terms of the different components of Fourier fields, which are the diffractions in different directions. E is the electric field, ε and μ is the permittivity and permeability, ω is the angular frequency b_i is the Fourier coefficient of different diffraction orders and $k_{x,i}$ is the corresponding x-component of the Fourier wavevector. E_{inc} is the incident electric field amplitude, and k_{inc} the incident field wavevector.

Therefore, the electric field is expanded as

$$E(x,z) = E_{inc} exp(jk_{inc} z) + \sum_i b_i(z) exp(jk_{x,i} x) \quad (2)$$

where the first term is the incident electric field, and the second term is the series expansion for the reflected electric field. i is the mode index and different modes correspond to power coupled into different directions.

In this section, the light scattering property is calculated for the silver metallic reflector and the white-paint diffuse medium reflectors. The specular power (0th order) and the diffused power (higher order) are calculated, and the diffused light scattering capability is then compared for these two reflectors. The incident medium is air in these calculations, to be consistent with the experimental setup in section 5. It should be emphasized that either far field or near field scattered power can be used to compare the scattering properties of different reflectors. In fact, the result and comparison will be very similar. In this section, the far-field angular emission power is used to distinguish the performance of metallic and dielectric reflectors.

From Fig. 3 and Fig. 4, the angular power spectrum for the specular reflected power and the first-order reflected power are plotted. It can be seen that the 0th order power, i.e. specular reflection, is the strongest, which is very common in most eigen mode or scattering problems. Nevertheless, higher order diffraction is the key for the efficient light trapping in solar cells, and it can be seen that diffuse medium reflectors realized by white paint is very efficient for this purpose. This is easier to see if diffused light scattering efficiency is compared. Diffused scattering efficiency (D.S.E.) is defined as the diffused reflection power divided by the total reflected power

$$\text{D.S.E.}(\lambda) = \frac{\sum_{i\neq 0} |b_i(z)|^2}{\sum_{all\, i} |b_i(z)|^2} = \frac{P_{diffuse}(\lambda)}{P_{total}(\lambda)} \quad (3)$$

where the diffused power is calculated by summation over all reflection orders except the 0th one. The averaged diffused scattering efficiency weighted by AM 1.5 solar spectrum (D.S.E._{avg}), is 0.298 for the silver reflector and 0.519 for the white paint diffuse medium reflector. Along the line of regular RCWA analysis, the 0th and the 1st order reflected power in Fig. 3 and Fig. 4 is expressed in terms of power fraction, i.e. the 0th or the 1st order reflected power divided by the total incident power. The diffused scattering efficiency (D.S.E.) is defined in Eq. (3), and it is expressed as the diffused reflected power divided by the total reflected power.

#222520 - $15.00 USD Received 6 Oct 2014; revised 28 Nov 2014; accepted 20 Dec 2014; published 26 Jan 2015

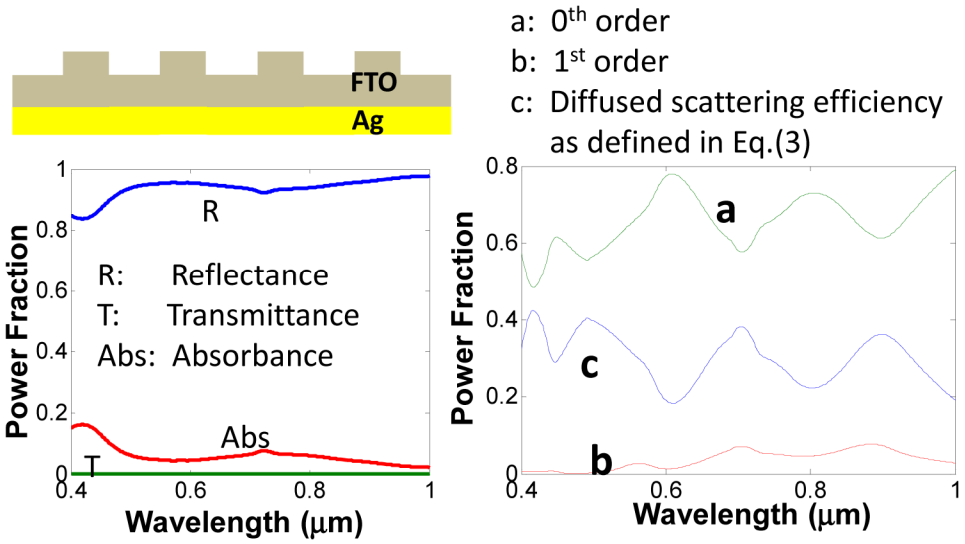

Fig. 3. The theoretical diffraction property for a silver metallic reflector. (Left)The total reflectance(R), absorbance(Abs), and transmittance(T). (Right) The diffused scattering efficiency (D.S.E.), the 0th order specular reflected power (0, 0), and the strongest diffused power which corresponds to the first-order diffraction (± 1, ± 1).

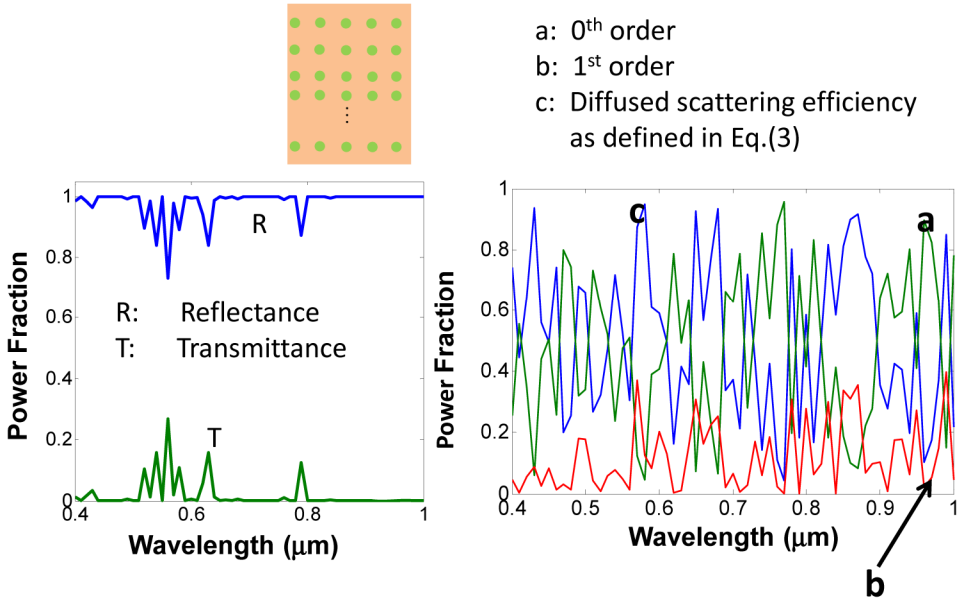

Fig. 4. The theoretical diffraction property for a white paint diffuse medium reflector. (Left)The total reflectance(R), absorbance(Abs), and transmittance(T). (Right) The diffused scattering efficiency (D.S.E.), the 0th order specular reflected power (0, 0), and the strongest diffused power which corresponds to the first-order diffraction (± 1, ± 1).

#222520 - $15.00 USD Received 6 Oct 2014; revised 28 Nov 2014; accepted 20 Dec 2014; published 26 Jan 2015

4. Experimental result for thin-film amorphous silicon solar cells

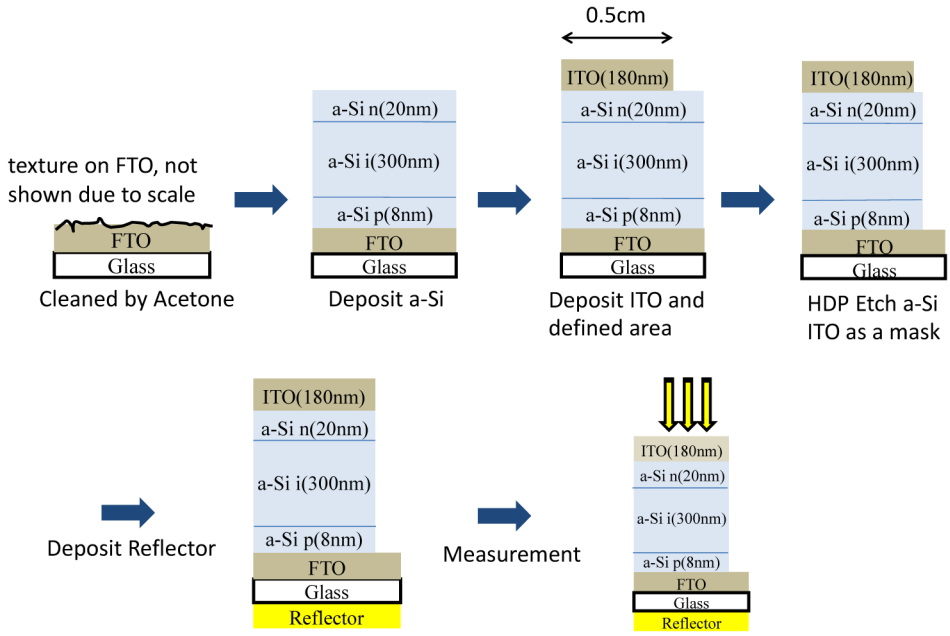

Fig. 5. The process steps for fabricating amorphous silicon thin-film solar cell using very-high-frequency plasma enhanced chemical vapor deposition (VHF-PECVD).

Fluorine-doped tin oxide (FTO) coated glass is cleaned by acetone firstly (see Fig. 5). Afterward, the p-i-n amorphous silicon film is deposited on FTO glass and the thickness of p, i, and n layers are 8nm, 300nm and 20nm, respectively. The p-i-n silicon film is deposited by very high frequency plasma-enhanced chemical vapor deposition (VHF-PECVD) at 250°C. The indium tin oxide(ITO) thickness is 180nm and is deposited by sputtering. A shadow mask is placed on top of α-Si:H during ITO deposition to form the patterned ITO electrodes. Since the white paint material currently used in this study is non-conducting, etching is necessary to make the ohmic contact to the bottom FTO layer which is in turn in contact with the p-type emitter. Therefore, reactive ion etching (RIE) using CF_4/Argon(Ar) at 20 mtorr is employed to etch the portion of silicon film which is not covered by ITO. This way the contact to the bottom FTO layer is achieved. Aluminum ohmic contact can be formed on the FTO and ITO layer, but based on our measurement, probe directly in contact with FTO or ITO leads to similar measurement result. For the white paint back reflector, the commercial white paint is applied at the back side of the glass substrate. It is confirmed with the vendor that the white paint is indeed TiO_2 pigments. According to the vendor, in their commercial paint products, they use mixed TiO_2 diameters ranging from 200nm-500nm. Therefore, in a specific paint, a mixture of TiO_2 particles with different sizes exists. The vendor uses mixture of varying-diameter pigments to enhance the broadband reflectance. Different products from this same vendor can have different proportions of different-sized pigments, in order to target at different spectral ranges. The exact proportion specifically for the paint used here is not disclosed, but based on its high reflectance in the visible spectrum, we believe that most of the TiO_2 particles are closer to the larger side, i.e. 500nm. In fact, we have been searching for different paints, and the one employed in this study is closest to our theoretical setup and result. Lab-synthesized white paints will be an important future direction.

For the metallic back reflector, evaporation is used to deposit metal on the back side of the glass substrate.

#222520 - $15.00 USD Received 6 Oct 2014; revised 28 Nov 2014; accepted 20 Dec 2014; published 26 Jan 2015

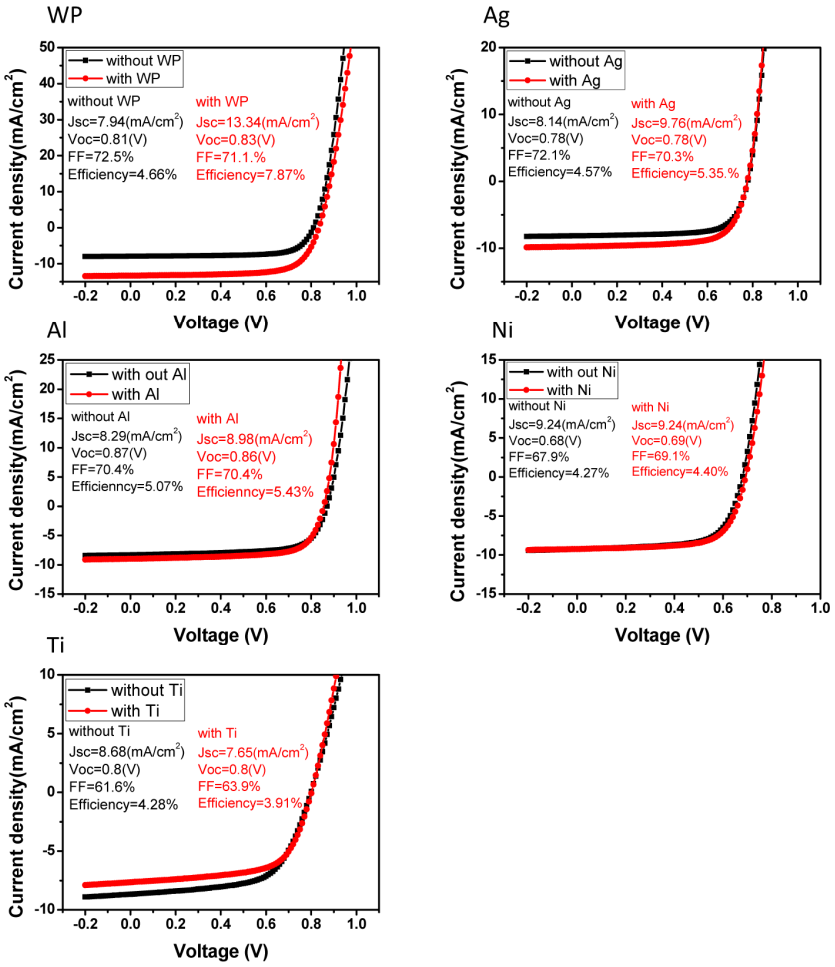

Fig. 6. The current-voltage characteristics (J-V) for the solar cells with various reflectors including white paint diffuse medium reflectors, silver, aluminum, titanium, and nickel.

In Fig. 6, J-V curve is measured for devices with metal or white-paint back reflectors applied to the back side of the FTO-coated glass substrate. The measurement is carried out using Keithley 2440 5A source meter, Oriel sol3A class AAA solar simulator, and Forter I-V measurement & analysis system. The device is 0.5cm × 0.5cm after dry plasma etching, and the substrate area is 1cm × 1cm.

Based on our experimental study, the efficiency enhancement using a white paint diffuse medium reflector is the highest among all reflectors (see Table 1). This can be attributed to its zero absorption loss and large angle light scattering evident from the theoretical result in section 3. It is, therefore, suggested that diffuse medium reflectors are, in fact, very promising, due to its zero absorption loss, low-cost, low-temperature process, and high throughput. From this experimental verification, it is demonstrated that the concept of diffuse medium reflectors can indeed be applied to future photovoltaics. It should be pointed out that by wave optics design and optimization in the pigment size/shape and in the pigment volume concentration (PVC), the reflectance and diffraction property of white-paint diffuse medium reflectors can be further improved in the future. In this case, a lab-synthesized paint, rather than commercial ones, is preferable, and the pigment size, shape, and PVC can therefore be controlled as desired.

#222520 - $15.00 USD Received 6 Oct 2014; revised 28 Nov 2014; accepted 20 Dec 2014; published 26 Jan 2015

Table 1. Comparison of relative enhancement in conversion efficiency(η) for different reflectors

Mirror Type	Diffuse Medium using White Paint	Ag	Al	Ni	Ti
Baseline, η	4.66%	4.58%	5.07%	4.27%	4.28%
w/ Reflector, η	7.87%	5.35%	5.43%	4.4%	3.91%
Relative Enhancement	68.88%	16.86%	7.1%	3.04%	–8.64%

5. Ultra-low specular emission for white-paint diffuse medium reflectors

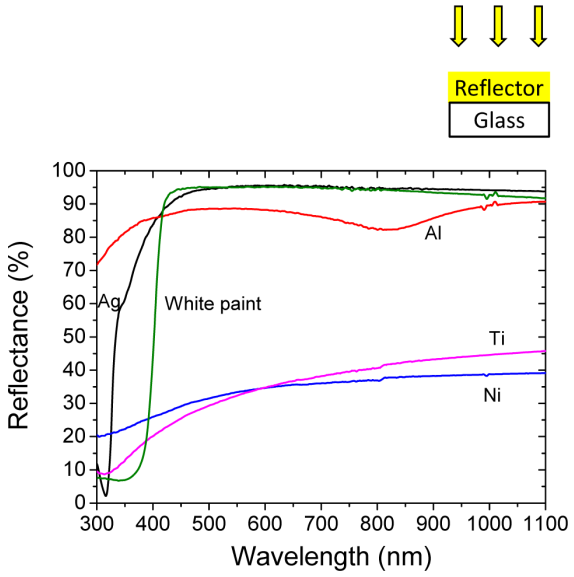

Fig. 7. The Ultraviolet–visible spectroscopy (UV-VIS) spectrum for the reflectance of various reflectors

Figure 7 is the Ultraviolet–visible spectroscopy (UV-VIS) measurement for various reflectors. Metallic and white-paint diffuse medium reflectors are coated on the glass, and UV-VIS spectrum is measured from 300nm to 1100nm. In this study, the composition of white paint is TiO_2 nanoparticles embedded in synthetic resin. In UV-VIS measurement, it is seen that the reflectance of the white-paint diffuse medium can actually be as high as silver. The promising result leads to the applicability to solar cells. In order to further study the angular reflection behavior for various metallic reflectors and diffuse medium white-paint reflectors, the angular measurement is conducted. The reflector structures of real solar cells in section 4 are used for the angular measurement. The texture on the dielectric with a planar metallic mirror is shown to be the most effective configuration for metal-backed solar cells [47]. This is because the texture on the metal itself tends to result in more metallic absorption loss even in the presence of a dielectric spacer. In Fig. 8, the specular and the diffused powers versus wavelength and angle are plotted for various reflectors. The specular power is measured directly, and the diffused power is calculated by subtracting the specular reflected power from the total reflected power. Measuring diffused power directly is also possible in our experimental set-up, but the accuracy can be worse. The total reflected power is measured using integration sphere at normal incidence. The specular reflected power is measured at a small incidence angle (20°) since at normal incidence the detector and the light source are on

#222520 - $15.00 USD Received 6 Oct 2014; revised 28 Nov 2014; accepted 20 Dec 2014; published 26 Jan 2015

the same line, and the specular power is difficult to measure. The diffused scattering efficiency (D.S.E.) is defined by Eq. (3), and the averaged value ($D.S.E._{avg}$) is the mean value of D.S.E. weighted by AM1.5 solar spectrum. It can be seen from Fig. 8 that the D.S.E. for the white paint diffuse medium reflectors are higher than **0.8** over the entire spectral range of interest for light trapping (600nm-1000nm). The titanium (Ti) has second high D.S.E. but its low reflectance makes it not useful for solar cell application. The experimental result is consistent with the theoretical results in section 3, using coupled mode theory. The superior large-angle diffraction property for white paint diffuse medium reflector results from the fact that the embedded nano-particles enhance the photon backward diffractions. The effect is significant, and it is potentially more efficient than plasmonic resonance, based on the experimental amorphous silicon solar cell result in section 4.

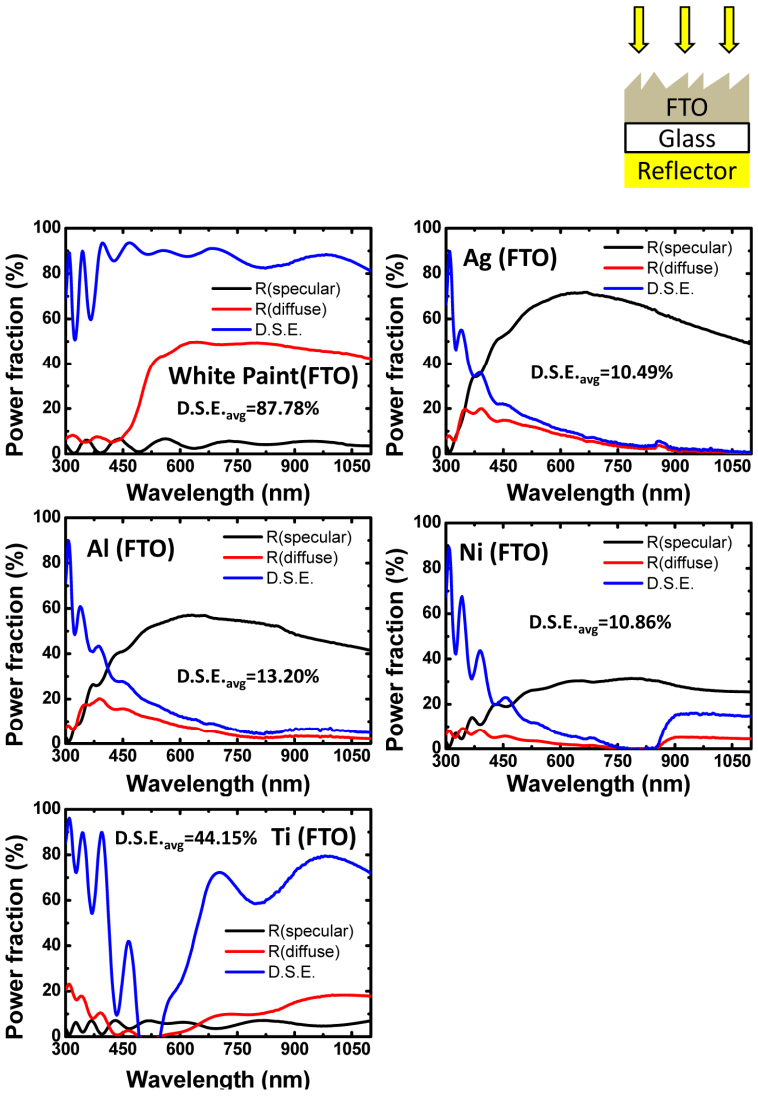

Fig. 8. The specular and diffused component of the reflected power for different reflectors. The structure for this specular and diffused power measurement is the back reflector structure in real solar cells in section 4. The diffused scattering efficiency (D.S.E.) is defined as the diffused power divided by total reflected power and it characterizes the reflectors' large-angle diffraction capability.

#222520 - $15.00 USD Received 6 Oct 2014; revised 28 Nov 2014; accepted 20 Dec 2014; published 26 Jan 2015

6. Conclusion

The white-paint diffuse medium reflectors are compared to different metallic reflectors with varying conductivity in order to achieve ultra-high efficiency photovoltaics. The theoretical result shows the diffuse medium reflectors possess superior light scattering property, despite the absence of surface plasmon excitation. The RCWA calculation shows that the diffracted power at non-specular direction, for diffuse medium reflectors, is significantly higher than its metallic counterparts. The fabrication of amorphous silicon solar cells with various back reflectors further confirms the feasibility and the superiority of diffuse medium reflectors for photovoltaics. The enhancement of short circuit current and efficiency is the most pronounced for white-paint diffuse medium reflectors, even compared to highly conductive silver reflectors. The high efficiency of solar cell with diffuse medium reflectors is attributed to the strongest angular diffraction and zero metallic absorption loss. The UV-VIS measurement reveals that the high reflectance of the diffuse medium can be comparable to silver (Ag), provided the optimal geometry of TiO_2 nanoparticles is employed. The measurement of specular and diffused power further confirms the superior light scattering property for the diffuse medium reflectors. It is seen that the diffused scattering efficiency (D.S.E.) provided by a diffuse medium reflector is much higher than its metallic counterparts. We propose that diffuse medium reflectors are very promising, and all-dielectric solar cell reflectors should be used for future photovoltaics employing nanophotonic light trapping.

#222520 - $15.00 USD Received 6 Oct 2014; revised 28 Nov 2014; accepted 20 Dec 2014; published 26 Jan 2015